

Loughborough University Institutional Repository

Investigation of the acoustic black hole termination for sound waves propagating in cylindrical waveguides

This item was submitted to Loughborough University's Institutional Repository by the/an author.

Citation: AZBAID EL OUAHABI, A., KRYLOV, V.V. and O'BOY, D.J., 2015. Investigation of the acoustic black hole termination for sound waves propagating in cylindrical waveguides. Presented at InterNoise 2015, 44th International Congress and Exposition on Noise Control Engineering, San Francisco, USA, 9-12 August.

Additional Information:

- This is a conference paper.

Metadata Record: <https://dspace.lboro.ac.uk/2134/18926>

Version: Accepted for publication

Publisher: © International Institute of Noise Control Engineering (I-INCE)

Rights: This work is made available according to the conditions of the Creative Commons Attribution-NonCommercial-NoDerivatives 4.0 International (CC BY-NC-ND 4.0) licence. Full details of this licence are available at: <https://creativecommons.org/licenses/by-nc-nd/4.0/>

Please cite the published version.



Investigation of the acoustic black hole termination for sound waves propagating in cylindrical waveguides

Abdelhalim Azbaid El-Ouahabi^{a)}

Victor V. Krylov^{b)}

Daniel J. O'Boy^{c)}

Department of Aeronautical and Automotive Engineering, Loughborough University
Loughborough, Leicestershire, LE11 3TU, UK

So far, acoustic black holes have been investigated mainly for flexural waves in thin plates for which the required linear or higher order reduction in wave velocity with distance can be easily achieved by changing the plate's local thickness. In the present paper, the results of the experimental investigations of the acoustic black hole for sound absorption in air are described. To achieve the required power-law decrease in sound velocity with propagation distance the inhomogeneous acoustic waveguides earlier proposed by Mironov and Pisyakov (2002) and made of quasi-periodic ribbed structures have been manufactured to provide linear and quadratic decreases in acoustic wave velocity with distance. Measurements of the reflection coefficients for guided acoustic modes incident on the black holes have been carried out in the frequency range of 100-1000 Hz. Initial measurements were conducted without insertion of any absorbing materials. The results show the possibility of significant reduction of the acoustic reflection in this case. Addition of small pieces of absorbing porous materials caused further reduction in the reflection coefficients, albeit not as significant as it could be expected.

1 INTRODUCTION

'Acoustic black holes' are new physical and engineering objects that can absorb almost 100% of the incident wave energy. This makes them attractive for applications in noise and vibration control¹⁻¹¹. The principle of operation of acoustic black holes is based on a linear or higher order power-law-type decrease in velocity of the incident wave with propagation distance to almost zero, which should be accompanied by efficient energy absorption in the area of low velocity via small pieces of inserted absorbing materials.

^{a)} email: A.Azbaid-El-Ouahabi@lboro.ac.uk

^{b)} email: V.V.Krylov@lboro.ac.uk

^{c)} email: D.J.Oboy@lboro.ac.uk

So far, acoustic black holes have been investigated mainly for flexural waves in thin plates for which the required gradual reduction in wave velocity with distance can be easily achieved by changing the plate local thickness according to a power law, with the power-law exponent being equal or larger than two¹². This principle, in combination with adding small amounts of absorbing materials, has been applied to achieve efficient damping of flexural waves in plate-like structures using both one-dimensional ‘acoustic black holes’ (power-law wedges and beams with their sharp edges covered by narrow strips of absorbing materials)^{1-7, 10} and two-dimensional ‘acoustic black holes’ (power-law-profiled pits with small pieces of absorbing materials attached in the middle)⁸⁻¹¹.

There are still very few investigations of acoustic black holes designed for absorption of sound in gases and liquids. Such acoustic black holes could be used to enhance acoustic absorption in traditional noise control¹⁰. This would allow developers to apply smaller amounts of absorbing materials, which could reduce masses of the acoustic absorbing devices. The main difficulty here is to materialise a linear or higher order power-law decrease in velocity of the incident sound wave down to zero. For that reason, the recently developed acoustic absorbers based on gradient index metamaterials¹³⁻¹⁵, in which zero values of sound velocity were not achieved, represent not acoustic black holes, but impedance matching absorbing devices.

The first theoretical paper on acoustic black holes for sound absorption in air was published by Mironov and Pislyakov¹⁶. It was proposed in that paper to use inhomogeneous acoustic waveguides with walls of variable impedance materialised via quasi-periodic ribbed structures to achieve the required linear decrease in acoustic wave velocity with propagation distance down to zero. No inserted absorbing materials were considered in that theoretical paper.

The first experimental investigation of acoustic black holes for sound absorption in air, based on the above-mentioned inhomogeneous acoustic waveguides¹⁶ with inserted pieces of sponge as absorbing materials, has been carried out in our previous work¹⁷. In the present paper, we report the results of further experimental investigations of acoustic black holes for sound absorption in air based on the same design, but using different absorbing materials and their configurations.

2 EXPERIMENTS

2.1 Manufacturing of the Experimental Samples

Based on the theory developed in the paper¹⁶, two different samples of acoustic black holes formed by quasi-periodic ribbed structures materialising walls of variable impedance have been designed and manufactured - to provide linear and quadratic decreases in acoustic wave velocity with distance respectively.

The first structure, shown in Fig. 1, has the waveguide inner radius described by a linear power law function of the distance x : $r(x) = \varepsilon_1 x^1$, it will be referred to as ‘Linear Acoustic Black Hole’ (LABH) in this paper. The second structure has the inner radius as a quadratic power law function of x : $r(x) = \varepsilon_2 x^2$, it will be referred to as ‘Quadratic Acoustic Black Hole’ (QABH). Here ε_1 and ε_2 are constants. Both LABH and QABH consist of cylindrical plastic tubes of inner radius $R=115\text{ mm}$ and length $L=255\text{ mm}$ sealed at one end with a thick wooden backing of 13 mm thickness. Inside the tubes, a number of solid ribs (rings) of 2 mm thickness are mounted quasi-periodically, the first rib (ring) being separated from the wooden backing by the distance $S_b = 9\text{ mm}$ (for LABH) and by the distance $S_b = 30\text{ mm}$ (for QABH).

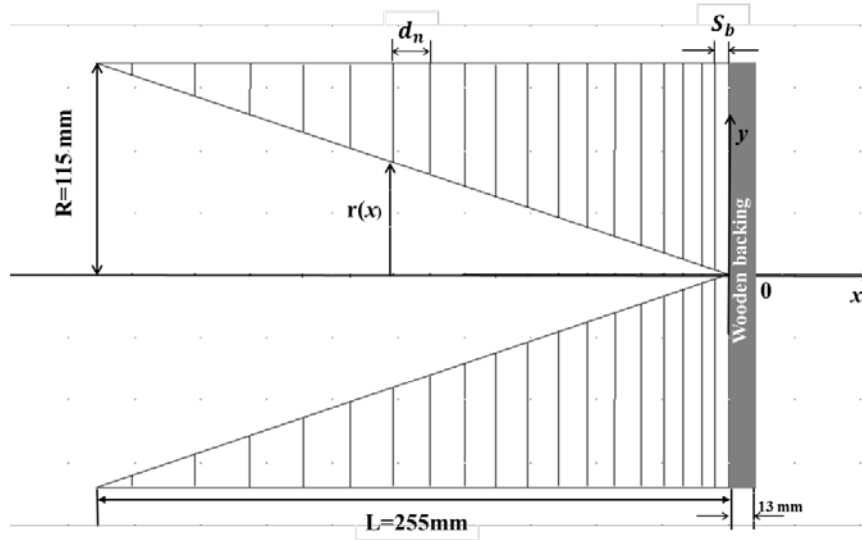


Fig. 1 – Schematic view of the manufactured Linear Acoustic Black Hole (LABH) showing the wooden backing and the distribution of the ribs whose inner radii decrease to almost zero.

The ribs (rings) have been made of laser cut steel in order to fit flush against the side of the tube wall, leaving no air gaps between the ribs' edges and the tube wall. The ribs for LABH and QABH were mounted with the increasing distances between them: $d_n = (3+n) \text{ mm}$ and $d_n = (6+n) \text{ mm}$ respectively, up to a maximum of 20 mm, where n is the rib number. These structures were expected to form the acoustic waveguides with varying wall admittances and varying cross sections. Inside the LABH and QABH, there were 18 ribs and 14 ribs respectively. Photographs of LABH and QABH are shown in the Figs. 2(a) and 2(b) respectively.

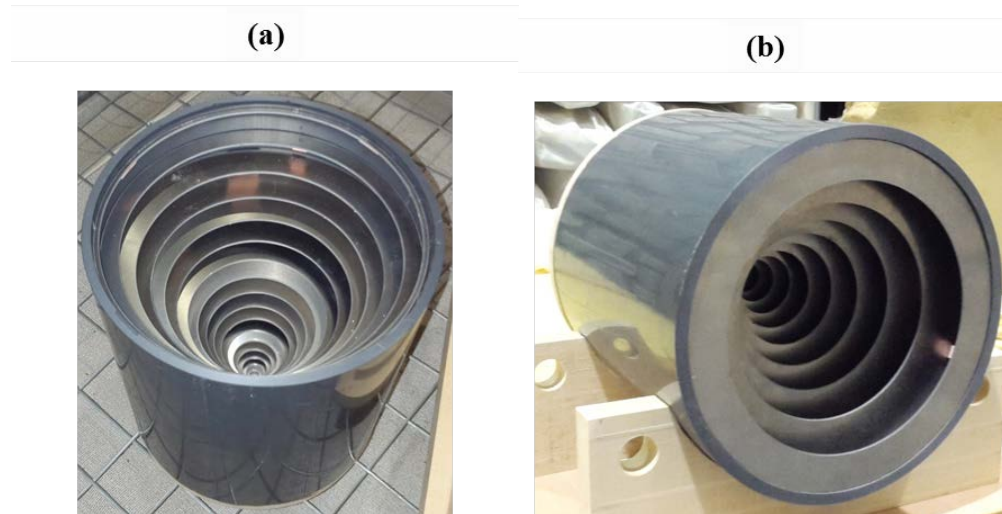


Fig. 2 – Photograph of LABH (a) and QABH (b)

2.2 Manufacturing of the Matching Impedance Tube

Based on the two microphone transfer function method, according to the standard procedure detailed in ISO 10534-2¹⁸, an impedance tube made of thick plastic has been designed and manufactured with the inner diameter close to those of the samples of acoustic black holes. This was done in order to measure the reflection coefficients of incident guided modes from the black holes only, and not from the jumps in tube diameters. The interior wall was smooth enough in order to maintain low sound attenuation for the lowest order guided modes (plane waves). A hard ring has been used to hold the black hole samples with the impedance tube. On the opposite end of the tube, a loudspeaker was fixed firmly, and an absorbent has been placed at the loudspeaker end of the tube to reduce the effect of resonances within the impedance tube. The length of the tube has to be long enough to ensure that plane waves are fully developed before reaching the microphones and the sample, and at least half of the longest wavelength can fit in it. Therefore, the length of the tube is $L_T = 1.5 \text{ m}$ and its inner diameter is $D_T = 225 \text{ mm}$.

Fourteen holes were drilled in the tube wall for positioning the measuring microphones, separated by 50 mm between them. The first hole was separated from one end of the tube by 50 mm. Those holes were drilled in order to enable measurements with different microphone positions and different separation between the input cross section of the sample and nearest microphone. Two holes have been used for positioning the microphones, the remaining holes had to be sealed in order to avoid air leakage into the tube. To achieve the low background noise, the tube must be sealed properly at all openings.

One of the important steps in using an impedance measurement tube is knowledge of the range of frequencies for which it will yield accurate results. Plane wave can be generated in a tube only if the excitation frequency is below the cut off frequency for the 2nd acoustic mode of the tube. This frequency can be determined as¹⁹:

$$f_u = \frac{0.58c}{D_T}, \quad (1)$$

where c is the speed of sound, and D_T is the tube diameter. Thus, the upper limiting frequency for the tube parameters used was $f_u = 884 \text{ Hz}$.

There are also restrictions on the microphone spacing¹⁹. In particular, the lower limiting frequency depends on the distance between the microphone positions, S_0 , which should be larger than 5 % of the longest measurable wavelength. Therefore, S_0 determines the lower limiting frequency f_l using the following condition:

$$f_l > \frac{0.05c}{S_0}. \quad (2)$$

Problems also rise, if the microphone spacing becomes too wide. This leads to an upper frequency limit due to microphone spacing given by:

$$f_u < \frac{0.45c}{S_0}. \quad (3)$$

For the selected distance $S_0 = 150 \text{ mm}$, it follows from (2) and (3) that $f_l > 114 \text{ Hz}$, and $f_u < 1092 \text{ Hz}$, the latter being larger than the above-determined $f_u = 884 \text{ Hz}$. Consequently, the useful frequency range for the constructed impedance tube is 114 – 884 Hz.

2.3 Experimental Setup

The two microphone transfer function method has been used in this work to measure the sound pressure reflection coefficients from the samples of the acoustic black holes. The experimental set-up comprised the impedance tube described above, a loudspeaker fixed at one end (it produced the constant broadband sound using a white noise generator), and two nominally identical microphones (GRAS 40E, pre-polarized ½ inch free-field). The microphones were calibrated via the same pistonphone, to measure the sound pressure. The two microphones were mounted flush with the inside wall of the tube, isolated from the tube to minimize sensitivity to vibration, and connected to a PC via a dynamic signal acquisition module NI-USB-4431 card (four analog input channels and one analog output channel) for making sound measurements. The selected spacing between the input cross section of the acoustic black holes and the nearest microphone and between the microphone positions were $L_0 = 200\text{mm}$ and $S_0 = 150\text{mm}$ respectively. Figure 3 shows the acoustic impedance tube with the microphones mounted on the tube. Shown are also the loudspeaker and the sample of acoustic black hole that is fixed to the end of the tube. The two microphone transfer function method was applied over a relatively large number of time samples, where the frequency response functions were processed to obtain the reflection coefficients from the two samples, LABH and QABH.

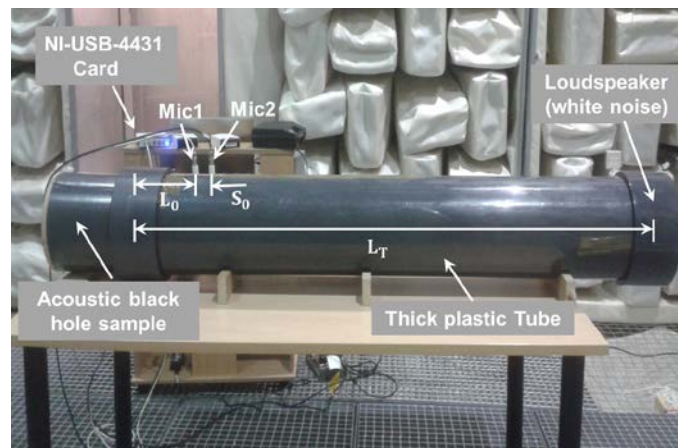


Fig. 3 – Photograph of the experimental set-up showing the impedance tube, two microphones mounted, a loudspeaker, the Acoustic black hole sample, and NI-USB-4431 Card: $L_T = 1.5\text{m}$, $D_T = 225\text{mm}$, $L_0 = 200\text{mm}$ and $S_0 = 150\text{mm}$

3 EXPERIMENTAL RESULTS AND DISCUSSION

Experimental measurements of the reflection coefficients for guided acoustic modes incident on the black holes (LABH and QABH) have been carried out in the frequency range of 100-1000 Hz. In the first instance, measurements were conducted without insertion of any absorbing materials. The results are shown in Figs. 4 and 5 by solid blue lines. One can see significant reductions in the reflection coefficients for both acoustic black holes in the frequency range of 100-874 Hz. Note that this frequency range is within the useful frequency range of the

constructed impedance tube. Comparison of the reflection coefficients results exhibited by LABH and QABH shows that the QABH is more efficient than LABH.

Following the ideas earlier implemented in acoustic black holes for flexural waves¹⁻¹¹, the additions of small pieces of sponge at the end of both samples have been made in our previous work¹⁷ in attempts to achieve further reduction in reflection coefficients. The results indeed showed some reduction in the reflection coefficients¹⁷ when the sponge was covering the cavity occupied by the first four ribs of LABH. However, this reduction was not as large as it could be expected. Therefore, other types of inserted porous absorbing materials and their configurations were to be tested. In the present work, two other types of absorbing material (fibreglass and mineral cotton) have been tested in both samples, covering the first four ribs. The results of the measurements of the reflection coefficients for both LABH and QABH are shown by dotted lines in Figs. 4 and 5 respectively.

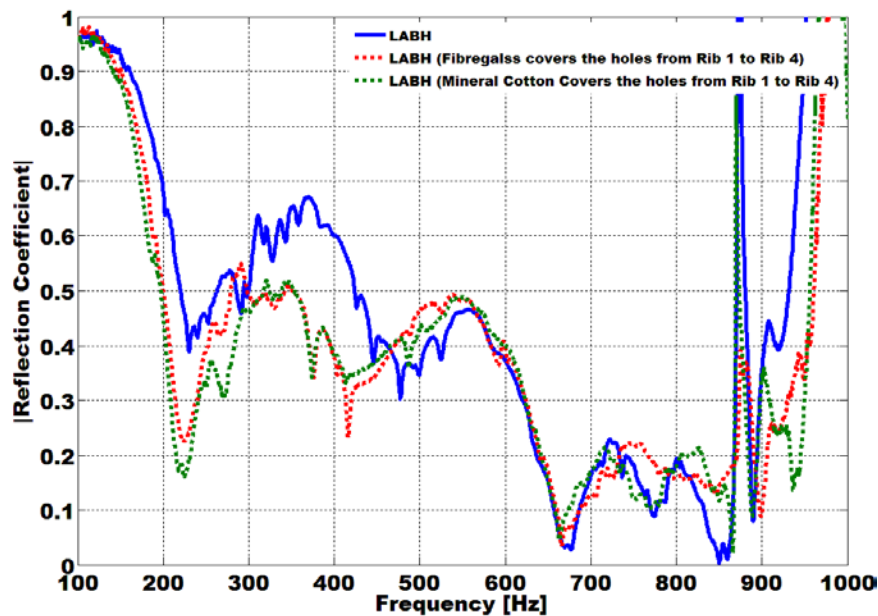


Fig. 4 – Frequency dependence of sound reflection coefficients from LABH (blue line), LABH (Fibreglass covers the holes of the first four ribs) (dashed red line), LABH (Mineral cotton covers the holes of the first four ribs) (dashed green line).

It can be seen from Fig. 4 that the applied porous absorbing materials, fibreglass and mineral cotton, that cover the space containing the first four ribs of LABH, cause further reduction in the reflection coefficients in the frequency range of 100 – 465 Hz. Out of that range, it seems to be not much difference between LABH with and without absorbing porous materials inserted. In the case of QABH (see Fig. 5), the curves of the reflection coefficients with and without inserted porous absorbing materials show similar behavior in the frequency range of interest.

Thus, the insertion of fibreglass and mineral cotton does not bring further significant reductions to the reflection coefficients for both samples, except for some reduction in the frequency range of 100 – 465 Hz in the case of LABH. These rather modest results stimulated

our attempts to use other configurations of absorbing materials to improve the efficiency of both devices and make it comparable with the case of acoustic black holes for flexural waves¹⁻¹¹.

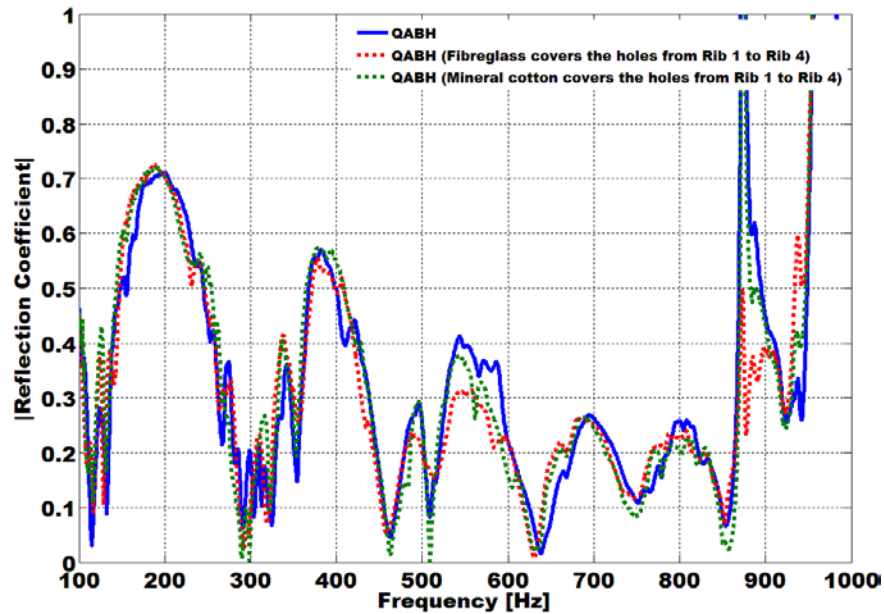


Fig. 5 – Frequency dependence of sound reflection coefficients from QABH (blue line), QABH (Fibreglass covers the holes of the first four ribs) (dashed red line), QABH (Mineral cotton covers the holes of the first four ribs) (dashed green line).

For this purpose, two and four thin strips of sponge have been glued in opposite sides on the circumference of the first rib holes, with the aim of gradual increasing the sound absorption in the area of slow velocity. The results of the measurements for both samples, LABH (two and four strips) and QABH (two and four strips), are shown in Figs. 6 and 7 respectively. It can be seen from Figs. 6 and 7 that thin strips of sponge glued inside of both acoustic black holes do not produce noticeable reductions in the reflection coefficients, unlike in the case of acoustic black holes for flexural waves¹⁻¹¹, where attachments of thin strips of absorbing materials result in dramatic reductions in flexural wave reflections.

4 CONCLUSIONS

In this paper, two samples of acoustic black holes for sound absorption in air, with linear and quadratic dependence of wave propagation velocity on distance respectively, have been tested experimentally. It has been shown that, if both experimental black holes are used without inserted porous materials, they reduce the sound reflection coefficients, and their frequency behaviour generally agrees with the theoretical predictions¹⁶. However, like in our previous work¹⁷, the insertion of porous absorbing materials, fibreglass and mineral cotton, does not bring further noticeable reductions to the sound reflection coefficients. Combinations of two and four strips of sponge have been inserted in attempts to achieve a more 'gentle' increase in acoustic absorption with distance. However, these strip configurations also did not show significant improvement. Further theoretical and experimental investigations should be carried out to clarify these issues and to achieve lower values of sound reflection coefficients.

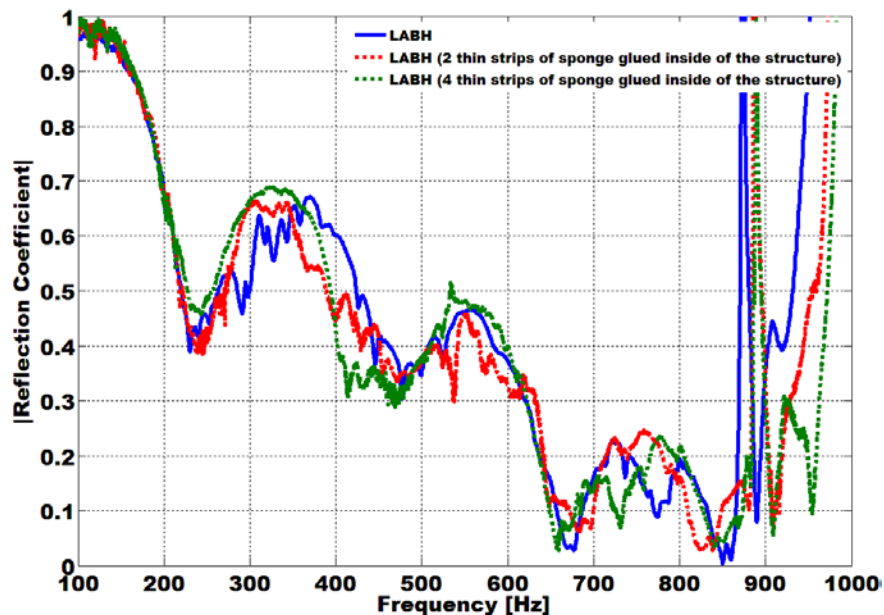


Fig. 6 – Frequency dependence of sound reflection coefficients from LABH (blue line), LABH (Two thin strips glued in opposite side on the circumference of the first rib holes) (dashed red line), LABH (Four thin strips glued in opposite side on the circumference of the first rib holes) (dashed green line).

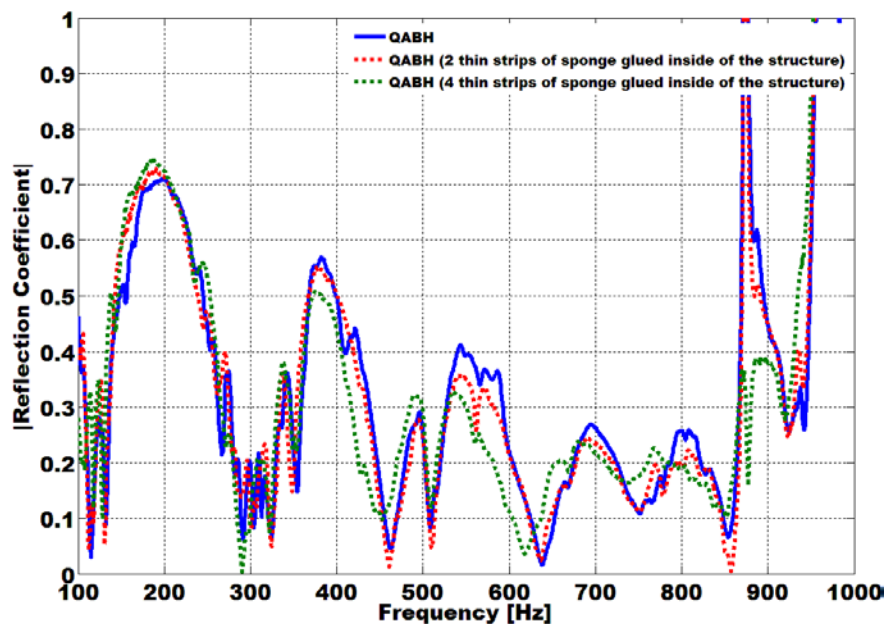


Fig. 7 – Frequency dependence of sound reflection coefficients from QABH (blue line), QABH (Two thin strips glued in opposite side on the circumference of the first rib holes) (dashed red line), QABH (Four thin strips glued in opposite side on the circumference of the first rib holes) (dashed green line).

5 ACKNOWLEDGEMENTS

The research reported here has been supported by EPSRC grant EP/K038214/1. The authors would like to thank Sean Dyche for his contribution to the design of the experimental acoustic black holes and Onkar Gill for his participation in the development of the experimental impedance tube.

6 REFERENCES

1. V. V. Krylov, "New type of vibration dampers utilising the effect of acoustic 'black holes'", *Acta Acustica united with Acustica*, **90**(5), 830–837, (2004).
2. V. V. Krylov and F. J. B. S. Tilman, "Acoustic 'black holes' for flexural waves as effective vibration dampers", *Journal of Sound and Vibration*, **274**, 605-619, (2004).
3. V. V. Krylov and R. E. T. B. Winward, "Experimental investigation of the acoustic black hole effect for flexural waves in tapered plates", *Journal of Sound and Vibration*, **300**, 43-39, (2007).
4. V. Kralovic and V. V. Krylov, "Damping of flexural vibrations in tapered rods of power-law profile: Experimental studies", *Proceedings of the Institute of Acoustics*, **29**(5), 66-73, (2007).
5. D. J. O'Boy, V. V. Krylov and V. Kralovic, "Damping of flexural vibrations in rectangular plates using the acoustic black hole effect", *Journal of Sound and Vibration*, **329**, 4672–4688, (2010).
6. J. J. Bayod, "Experimental study of vibration damping in a modified elastic wedge of power-law profile", *Journal of Vibration and Acoustics*, **133**, 061003 (2011).
7. V. Denis, A. Pelat, F. Gautier and B. Elie, "Modal Overlap Factor of a beam with an acoustic black hole termination", *Journal of Sound and Vibration*, **333**, 2475-2488 (2014).
8. V. B. Georgiev, J. Cuenca, F. Gautier, L. Simon and V. V. Krylov, "Damping of structural vibrations in beams and elliptical plates using the acoustic black hole effect", *Journal of Sound and Vibration*, **330**, 2497–2508, (2011).
9. E. P. Bowyer, D. J. O'Boy, V. V. Krylov and F. Gautier, "Experimental investigation of damping flexural vibrations in plates containing tapered indentations of power-law profile", *Applied Acoustics*, **74**(4), 553-560, (2013).
10. V. V. Krylov, "Acoustic black holes: Recent developments in the theory and applications", *IEEE Transactions on Ultrasonics, Ferroelectrics, and Frequency Control*, **61** (8), 1296-1306, (2014).

11. S. C. Conlon, J. B. Fahnlone and F. Semperlotti, "Numerical analysis of the vibroacoustic properties of plates with embedded grids of acoustic black holes", *Journal of the Acoustical Society of America*, **137** (1), 447-457 (2015).
12. M. A. Mironov, "Propagation of a flexural wave in a plate whose thickness decreases smoothly to zero in a finite interval", *Soviet Physics – Acoustics*, **34**, 318-319, (1988).
13. A. Climente, D. Torrent and J. Sanchez-Dehesa, "Omnidirectional broadband acoustic absorber based on metamaterials", *Applied Physics Letters*, **100**, 144103, (2012).
14. O. Umnova and B. Zajamsek, "Omnidirectional graded index sound absorber", *Proceedings of the Conference 'Acoustics 2012'*, Nantes, France, 23-27 April 2012, 3631-3637, (2012).
15. A. Azbaid El-Ouahabi, V. V. Krylov and D. J. O'Boy, "Quasi-flat acoustic absorber enhanced by metamaterials", *Proceedings of Meetings on Acoustics* **22**, 040002, (2014).
16. M. A. Mironov and V. V. Pislyakov, "One-dimensional acoustic waves in retarding structures with propagation velocity tending to zero", *Acoustical Physics*, **48** (3), 347-352, (2002).
17. A. Azbaid El-Ouahabi, V. V. Krylov and D. J. O'Boy, "Experimental investigation of the acoustic black hole for sound absorption in air", *Proceedings of 22nd International Congress on Sound and Vibration*, Florence, Italy, 12-16 July 2015 (to appear).
18. ISO 10534-2, "Acoustics –Determination of sound absorption coefficient and impedance in impedance tube – Part 2: Transfer-function method", (1998).
19. T. J. Cox and P. D'Antonio, *Acoustic Absorbers and Diffusers: Theory, design and application*", 2nd Edition, Taylor & Francis, Oxford, (2009).